Author/s:
Xiang, R;Breen, E;Bolormaa, S;Liu, Z;Vander Jagt, CJ;Dong, M;Lindblad-Toh, K;Rochfort, S;Pryce, JE;Chamberlain, AJ;Goddard, ME

Title:
Integrating extensive functional annotations and multiomics of cattle enhances climate resilience prediction and mapping

Date:
2025-12-09

Citation:
Xiang, R., Breen, E., Bolormaa, S., Liu, Z., Vander Jagt, C. J., Dong, M., Lindblad-Toh, K., Rochfort, S., Pryce, J. E., Chamberlain, A. J. & Goddard, M. E. (2025). Integrating extensive functional annotations and multiomics of cattle enhances climate resilience prediction and mapping. Proceedings of the National Academy of Sciences of the United States of America, 122 (49), pp.e2514736122-. https://doi.org/10.1073/pnas.2514736122.

Persistent Link:
https://hdl.handle.net/11343/368091

PNAS RESEARCH ARTICLE | AGRICULTURAL SCIENCES OPEN ACCESS

Integrating extensive functional annotations and multiomics of cattle enhances climate resilience prediction and mapping

Ruidong Xiang[a,b,c,d,1], Edmond Breen[a], Sunduimijid Bolormaa[a], Zhiqian Liu[a], Christy J. Vander Jagt[a], Michael Dong[e,f], Kerstin Lindblad-Toh[e,f,g], Simone Rochfort[a,b], Jennie E. Pryce[a,b], Amanda J. Chamberlain[a,b], and Michael E. Goddard[a,c]

Affiliations are included on p. 9.

Edited by William Murphy, Texas A&M University, College Station, TX; received June 7, 2025; accepted October 2, 2025

To understand the biological function of genomic regions, vast molecular data have been generated to annotate mammalian genomes. However, how to effectively use such extensive information to improve the mapping and prediction of complex traits, including those that respond to climate change, remains unresolved. Here, we apply a Bayesian framework to estimate a Functional-And-Evolutionary Multi-trait Importance (FAEMI) score that combines extensive functional annotations to predict the probability that a variable genomic site causes variation in 16 complex traits of 103 K cattle. The functional annotations include information from the transcriptome, epigenome, and metabolome of cattle as well as genome constraints across species from multiple genome annotation consortia, covering 2.13 million molecular phenotypes from 24 tissues/cell types of 8,446 cattle worldwide. FAEMI analyses quantify the phenotypic importance of functional assays to guide future annotation efforts and reveal significant correlations between molecular functionality and genotype-to-phenotype associations. In new data of 45 K cattle with heat tolerance phenotypes, the FAEMI score demonstrates significant advantages in improving genomic prediction and mapping. The FAEMI score improved genomic prediction accuracy of multiple heat tolerance phenotypes by ~11%. A cellular stress-related locus, stress-associated endoplasmic reticulum protein family member 2 (*SERP2*), was identified as underlying heat tolerance, with the lead variant (rs383130643) associated with enhancer activity. Additionally, high FAEMI-ranking variants are significantly enriched in variants affecting beef cattle traits. Together, our work provides methods and resources to map informative variants genome-wide, enhancing our understanding of the biology behind thermal tolerance and helping breed resilient cattle in a hotter world.

genomic prediction | multi-omics | heat tolerance | cattle | functional annotation

Significance

Ongoing work in functional annotations of genomes has generated rich datasets. We propose a method to link extensive functional annotations to genotype-to-phenotype associations. This method ranks annotation categories based on their contributions to phenotypes, which helps design future annotation experiments. It also estimates a score to rank all variants based on their functional, evolutionary, and phenotypic importance. We apply this score to new data on cattle heat tolerance and compare its performance against scores generated elsewhere. Our score shows robust performance in improving genomic prediction of heat tolerance traits and can help identify causal candidate genes. Our work provides new data and a framework for using functional information to improve the mapping and prediction of complex traits.

Many significant traits in evolution, medicine, and agriculture are determined by a large number of mutations and environmental effects, i.e., complex traits. Genome-wide association studies (GWAS) (1), especially at the sequence variant level, have identified many associations between single-nucleotide polymorphisms (SNPs) and complex traits (2). GWAS have also been extended to identify widespread pleiotropy, i.e., variants associated with multiple traits, in mammals (3, 4). However, as GWAS tests variant effects one at a time and there is extensive linkage disequilibrium (LD) in animals, most GWAS have failed to prioritize causal variants. Therefore, methods jointly analyzing variants, e.g., Bayesian mixture models, (5, 6) have been developed to improve mapping and genomic prediction.

Recently, studies have shown that variants with some functional annotations are enriched for associations with phenotypes, and therefore, the functional annotations help to identify variants with effects on phenotype (7–11). For instance, the cattle Functional-And-Evolutionary Trait Heritability or FAETH score (8) was developed using data from ~44,000 cattle as well as functional datasets from a small number of individuals (N < 350). However, due to the analytical constraints, each trait and functional category was analyzed one at a time in the FAETH analysis. Another noticeable study is Wang et al. (10) where the authors trained Random Forest machine learning models based on expression quantitative trait loci (eQTLs) to predict genotype-to-phenotype associations in humans (10). However, the study was limited to eQTL annotations. In short, previous studies cover limited types of functional annotations, and none of these prior studies have analyzed traits relevant to environmental challenges, which are critical to agriculture and human health.

There is significant concern that the rising global temperature threatens agricultural and cattle productivity (12). The heat tolerance phenotypes of cattle, broadly defined as resistance to productivity decline in a hot environment, are complex traits with significant genetic components (13, 14). The biology behind heat tolerance of the host is unknown, but it has been assumed to be linked to cellular, morphological (e.g., coat color), behavioral, as well as neuro-endocrine systems (15). Selective breeding of cattle that can adapt to the changing

Author contributions: R.X. and M.E.G. designed research; R.X. performed research; R.X., Z.L., M.D., K.L.-T., S.R., J.E.P., and A.J.C. contributed new reagents/analytic tools; R.X., E.B., S.B., C.J.V.J., A.J.C., and M.E.G. analyzed data; and R.X., A.J.C., and M.E.G. wrote the paper.

The authors declare no competing interest.

This article is a PNAS Direct Submission.

[1]To whom correspondence may be addressed. Email: ruidong.xiang@agriculture.vic.gov.au.

This article contains supporting information online at https://www.pnas.org/lookup/suppl/doi:10.1073/pnas.2514736122/-/DCSupplemental.

Published November 24, 2025.

environment will significantly benefit agriculture. Here, we combined functional annotations with Bayesian mixture models (16) to analyze large datasets of cattle heat tolerance to enhance genomic mapping and prediction of heat resistance.

In the current study, we carried out a multitrait Bayesian analysis to estimate the probability that each variant affects one or more of 16 traits. Then, we used a regression analysis to predict this probability from a wide list of functional and evolutionary annotations. The functional and evolutionary annotations for the cattle genome were derived from our summary data from 8,446 cattle, predicted deleterious mutations in humans (17), three global consortia of genome annotation [Animal QTL database (18), FAANG (19), FarmGTEx (20)], 2.13 million quantitative molecular traits covering the transcriptome, epigenome, and metabolome from 24 tissues/cell types, and sequence data from 81 cattle breeds/subspecies (1,000 Bull Genome (21, 22)) and 305 vertebrates, mammals, and primates [Zoonomia project (23), Dataset S1]. The regression equation generates a score (the FAEMI score) that predicts the probability that each of 16 million variants affects one or more of the phenotypes (publicly available at https://figshare.unimelb.edu.au/articles/dataset/Functional-And-Evolutionary_Multi-trait_Importance_FAEMI_score_for_16_million_sequence_variants/27160245?file=58912450 with detailed explanation and tutorials). Finally, we use the FAEMI score in the analysis of new data on heat tolerance of 45 k cattle. We found that the FAEMI score not only increases the accuracy of the polygenic prediction or genomic selection of cattle heat tolerance but also identifies novel candidates for potential future intervention. Additional validation analyses in beef cattle data also show that high-ranking FAEMI variants are significantly enriched in QTL for beef carcass traits.

Results

Analysis Overview. To understand the phenotypic importance of functional information, we performed a stepwise analysis. First, Bayesian multitrait analyses (24) were applied to 16 decorrelated traits from 103 K Australian cows. These traits were daughter trait deviations, related to milk production, mastitis, fertility, temperament, and body conformation (Fig. 1 and Dataset S2 and *Methods*). The multitrait posterior inclusion probability (PIP_{mt}) was estimated for each of the 5.3 million variants (pruned variants from the total 16 million variants with linkage disequilibrium [LD]-r^2 >0.995 in 1 Mb windows), representing the probability of a variant affecting one or more of the 16 traits analyzed. Second, PIP_{mt} was regressed on the functional and evolutionary annotations to rank their phenotypic importance while accounting for minor allele frequency (MAF), LD and SNP density (Fig. 1 and *Methods*). The importance of annotations affecting PIP_{mt} was confirmed by repeating the analysis in 9 k bulls. Third, the multiple regression formula was used to estimate the probability (score) that each of the 16 million variants affected phenotypes based on their functional and evolutionary annotations. This score is called Functional-And-Evolutionary Multi-trait Importance (FAEMI) score; these are publicly available at https://figshare.unimelb.edu.au/articles/dataset/Functional-And-Evolutionary_Multi-trait_Importance_FAEMI_score_for_16_million_sequence_variants/27160245?file=58912450. Fourth, the FAEMI score was used to categorize those 16 million variants into 5 strata and multitrait BayesRC genome-wide fine-mapping was performed to verify the pleiotropic effects of the FAEMI ranking. As an external validation, in a new dataset, we compared the accuracy of predicting heat tolerance phenotypes for variants with high and low FAEMI scores. We also compared the performance of multiple linear regression trained FAEMI score against Random Forest training, our previous FAETH score (8) and random variants.

Phenotypic Importance of Functional and Evolutionary Categories. A wide variety of functional and evolutionary annotations were used so that 84% (13,471,657) of analyzed sequence variants segregating in 103 K Australian cows had at least one type of functional and/or evolutionary annotation. On average, each variant had 2 functional and/or evolutionary annotations (Fig. 2*A*). For variants with PIP_{mt} > 0.1, the top 5,001 variants, there was a tendency for variants

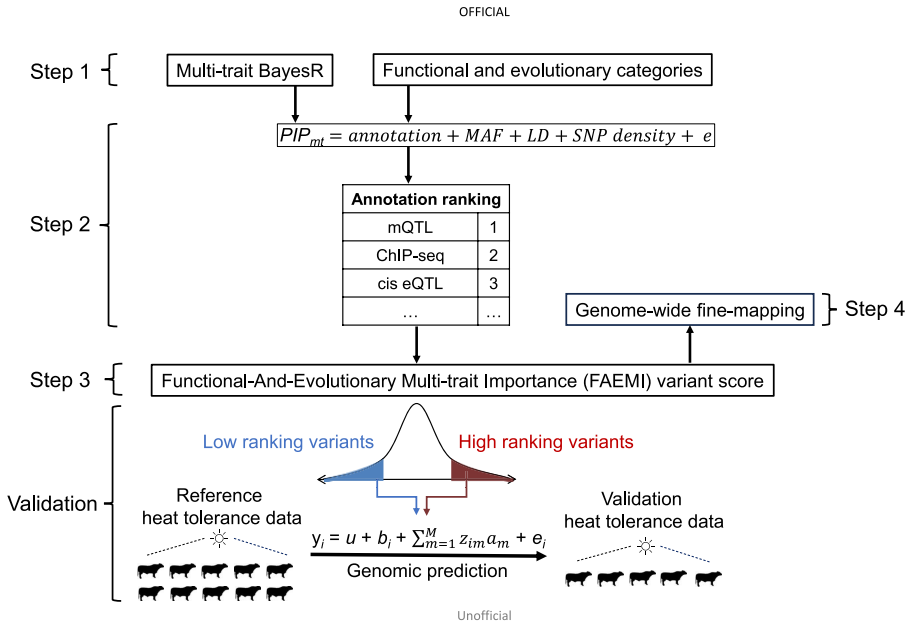

Fig. 1. Overview of the analysis. We first used multitrait BayesR to estimate the probability of variants having multitrait effects (Posterior Inclusion Probability or PIP_{mt}). Then, PIP_{mt} was regressed on functional and evolutionary classes. The result was used to rank ~50 functional categories (Dataset S1) and then to estimate a Functional-And-Evolutionary Multi-trait Importance (FAEMI) score to rank all variants analyzed. FAEMI score was also used in genome-wide fine mapping. In an external validation, we divided variants into high- and low-FAEMI variant sets and then used these variant sets to predict heat tolerance phenotypes (not used in training FAEMI score).

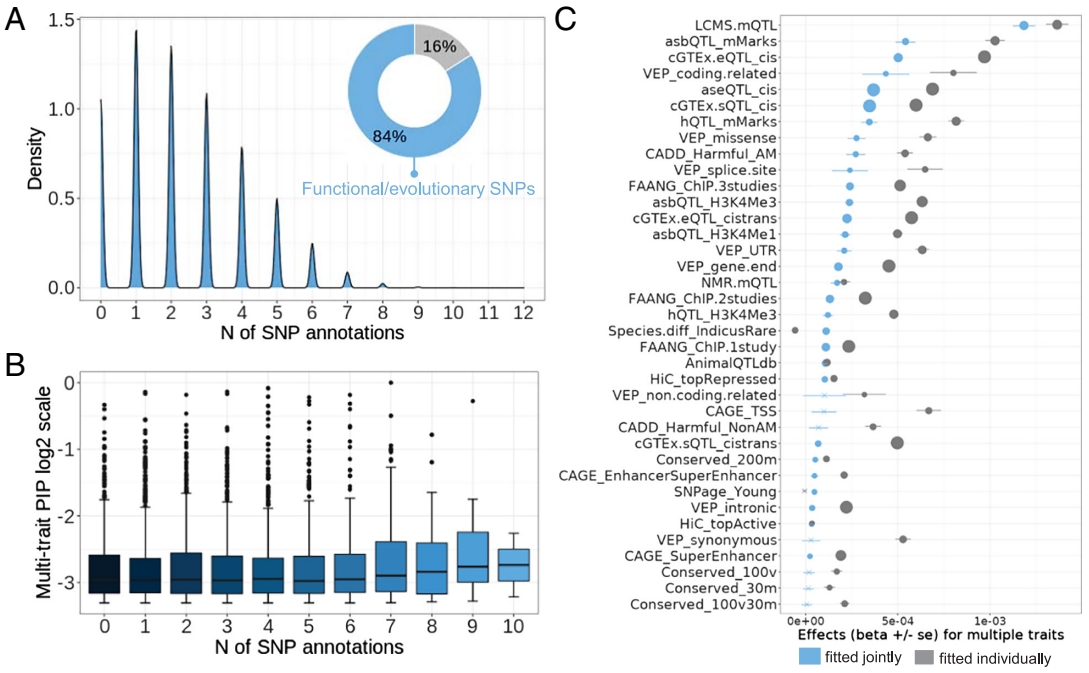

Fig. 2. Functional and evolutionary classes and their multitrait effects. (*A*) Distribution of sequence variants based on the number of functional and evolutionary annotations (x-axis). (*B*) Distribution of multitrait posterior inclusion probability (PIP_{mt}) across variants with different numbers of functional and evolutionary annotations. (*C*) Ranking of functional and evolutionary classes based on their effects on PIP_{mt}. The Y-axis labels are annotated as class_level with the details of functional and evolutionary classes found in Dataset S1. Functional categories were fitted together in one model (blue) or individually (gray). The order of functional categories from *Top* to *Bottom* is based on the effects estimated jointly. Crosses indicate the effects of functional categories that were not significant ($P \geqq 0.05$). The size of the circles reflects the −log10 of the *P*-value for their effects on PIP_{mt}.

with more functional and evolutionary annotations to have higher PIP_{mt} (Fig. 2*B*).

FAEMI analysis allowed us to rank the multitrait importance of all functional and evolutionary classes included (Fig. 2*C*). As shown in *SI Appendix*, Fig. S1, the correlation of phenotypic effects between the analyses fitting MAF, LD, and SNP density and not fitting MAF, LD, and SNP density was 0.99. However, whether all classes were fitted jointly or one at a time did significantly affect their effect on PIP_{mt} (Fig. 2*C*). Overall, fitting all classes jointly reduced their effects compared to fitting classes individually, indicating that some of the annotations were correlated and partially explained the same effects. For instance, the phenotypic effects of synonymous variants were large and significant when analyzed alone but became small and insignificant after fitting all classes jointly, suggesting their importance was largely explained by other annotations.

Consistent with our previous findings (8), liquid chromatography-mass spectrometry LCMS-based metabolite QTL (LCMS-mQTLs, 56 traits) had the strongest multitrait importance. This was followed by several sets of variants related to coding sequence and genetic and/or epigenetic regulation, including allele-specific-binding QTL (asbQTLs) in blood and *cis* gene expression QTL (eQTLs) from 16 tissues of the Cattle GTEx (20, 25, 26) and variants annotated by Variant Effect Predictor (VEP) (27) related to protein coding (VEP_coding.related). This was followed by allele-specific-expression QTL (aseQTL) from blood, milk cells, liver, and muscle, Cattle GTEx *cis* splicing QTLs (sQTLs), histone QTLs (hQTLs) (28) across multiple marks (H3K27ac, H3K4Me1, and H3K4Me3) measured by ChIP-seq from mammary gland, variants annotated as missense (VEP_missense), and variants predicted as deleterious mutations by the human CADD score (value $\geqq$ 20, CADD_Harmful_AM where AM meant the alleles are matched between cattle and human) (29). This set of variants was followed by variants annotated as being within splicing sites (VEP_splice.site) and variants annotated as under ChIP-seq peaks in 3 out of 4 FAANG (30–33) studies (FAANG_ChIP.3studies).

Metabolic profiles can also be quantified by NMR, and we have included another set of mQTLs derived from NMR (NMR-mQTLs, see *Methods*). This set of mQTLs was the result of association mapping 1,688 liver metabolites, and they showed significant effects on multiple traits, although the effect of NMR-mQTLs was smaller than the effect of LCMS-mQTLs. Chromatin architecture annotations based on Hi-C (*Methods*) were also investigated, and we found that variants within the A/B compartment-derived (34, 35) top active and repressed regions had significant pleiotropic effects. We also included enhancers and super-enhancers, annotated with Capped Analysis of Gene Expression (CAGE), from 12 tissues, and variants annotated as such showed significant multitrait effects. In addition, we confirmed that variants within regions annotated by the Animal QTL database (18) as associated with a wide variety of cattle complex traits had significant multitrait effects in this study.

Bos taurus taurus and *Bos taurus indicus* are two major subspecies of cattle that diverged ~0.5 Mya ago. We found that variants rare (MAF < 0.05) in *Bos taurus indicus* had significant pleiotropic effects, compared to variants common in *Bos taurus taurus* (MA $\geqq$ 0.1), variants common in *Bos taurus indicus* (MAF $\geqq$ 0.05) and random variants. Variants at sites conserved across 200 mammals also had significant multitrait effects, but variants conserved between 100 vertebrates or 30 mammals did not. Young variants had small but significant ($P = 0.0037$) effects on the traits analyzed.

We have also analyzed other variants with functional and/or evolutionary significance, including variants significant for 110 traits in the UK Biobank (36, 37), in predicted conserved brain enhancers (38), in selection signatures between beef and dairy cattle and sites conserved across species (Dataset S1 and *Methods*). Because these sets of variants did not show stronger pleiotropic effects than those of random variants, they were excluded from

the current study. Interestingly, the phenotypic effects of conserved sites were significant when analyzed alone. After fitting them jointly with other classes, only the effect of variants conserved across 200 mammals maintained significance.

To verify our results, we repeated the above analysis carried out in cows in data from 9 k bulls with the same 16 traits (*Methods*). We conducted 16-trait BayesR analyses in these bulls and then regressed the PIP_{mt} from bulls on functional and evolutionary classes. We then checked the correlation of the effects (regression coefficients) of functional and evolutionary classes between the bull analysis and the cow analysis (*SI Appendix*, Fig. S2). Although the effects in the bull analysis had a much smaller magnitude due to the smaller sample size, the correlation of phenotypic effects of functional and evolutionary classes between bulls and cows was 0.87, supporting the robustness of our analyses.

Functional-and-Evolutionary Multi-Trait Importance or FAEMI Score. The regression coefficients of ~50 functional and evolutionary classes were used to derive the FAEMI score for all 16 million variants based on their membership in different classes and the predicted probability of affecting multiple traits (Fig. 1). The FAEMI score was used to divide the 16 M variants into 5 strata from lowest to highest FAEMI score. Not surprisingly, the highest FAEMI stratum was enriched with variants identified as QTLs associated with multiple molecular phenotypes (e.g., eQTL, sQTL, hQTL, aseQTL, and asbQTL) or identified as predicted deleterious mutations by CADD score (Fig. 3*A*). To verify the phenotypic effects of FAEMI score, we conducted a 16-trait BayesRC analysis fitting 5 strata of variants based on the FAEMI ranking (*Methods*). We found these 5 strata had significantly different PIP_{mt} enriched with variants identified as QTLs associated with multiple molecular phenotypes (e.g., eQTL, sQTL, hQTL, aseQTL, and asbQTL) or identified as predicted deleterious mutations by CADD score (Fig. 3*A* and *SI Appendix*, Fig. S3). In fact, the differences between the strata in PIP were 10 times bigger than the FAEMI score predicted (Fig. 3*B*). This occurred because in BayesR all variants are assumed to be drawn from the same mixture of variant effects, whereas in BayesRC each strata has its own mixture of effect sizes.

Multitrait BayesRC genome-wide fine-mapping prioritized 415 variants ($PIP_{mt} \geqq 0.25$ (25, 40), Fig. 3*C*) for the 16 cattle traits. Of note, 15 out of 415 variants were orthologs of predicted deleterious mutations by CADD (Fig. 3*D* and Dataset S3). These mutations are recorded as rare disease mutations with low frequency in humans [MAF < 0.01, dbSNP (41) recording], but are common in Australian cattle (N = 103 K) with an average MAF of 0.14 (SD = 0.15, Dataset S3). Many of these mutations are also annotated as affecting gene regulation (Fig. 3*D*), including a regulatory variant (Chr14:64454721 or rs445616049) within gene *VPS13B*, whose human ortholog has been associated with Cohen syndrome (developmental disorder with obesity phenotypes). In cattle, the variant increases milk yield, protein yield, and survival and reduces fat, infertility, and gestation length (Fig. 3*D*). These results suggest that these human-cattle conserved genomic sites significantly affect

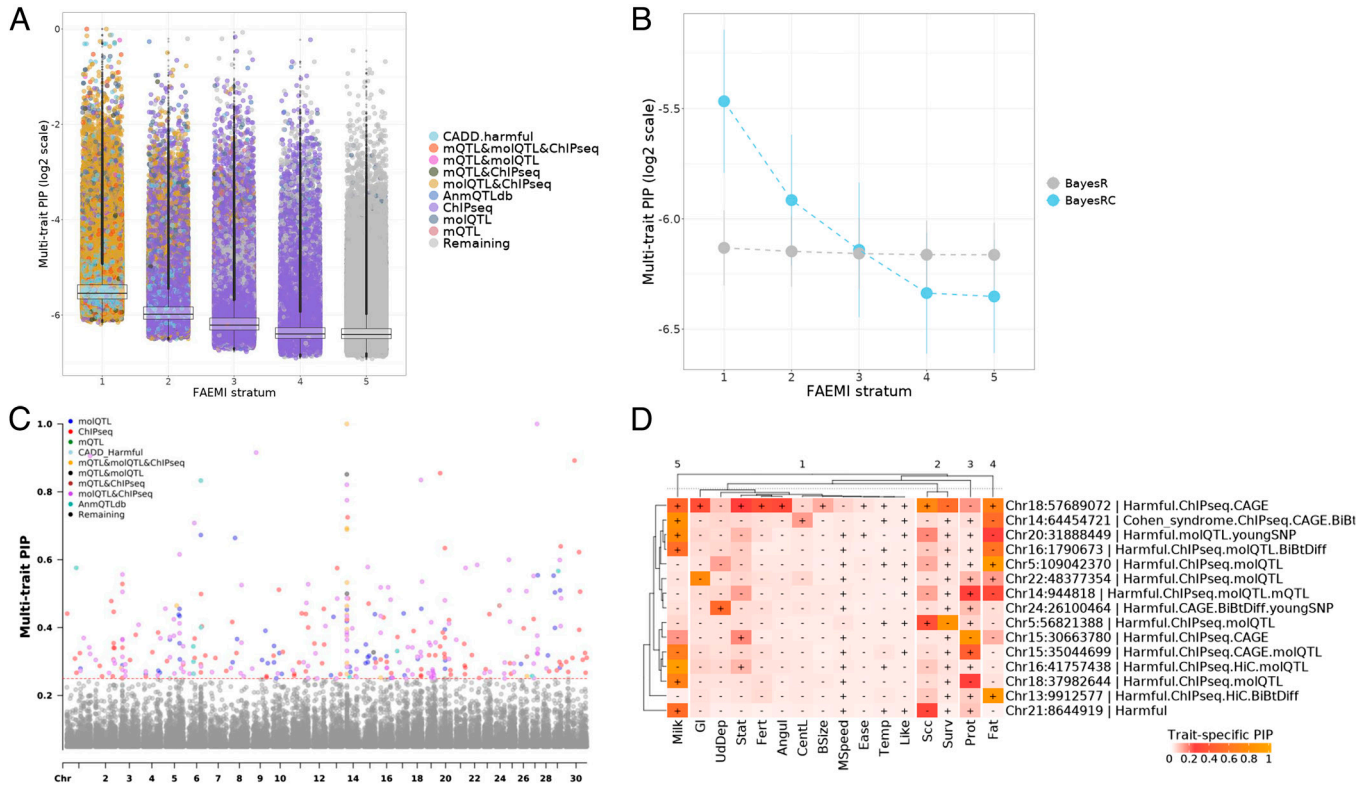

Fig. 3. FAEMI categories and pleiotropic effects. (*A*) Distribution of pleiotropic effects across 16 traits (PIP_{mt}) across 5 FAEMI strata. mQTL are metabolic QTL; molQTL are variants that are one or more type of eQTL, sQTL, hQTL, aseQTL, and asbQTL; ChIPseq are variants under one or more ChIP-seq mark; AnmQTLdb are variants associated with cattle complex traits from Animal QTL database. (*B*) Comparison of the distribution of pleiotropic effects between BayesR and BayesRC across 5 FAEMI strata. Dots represent means, and error bars represent SD. (*C*) Manhattan plot of cattle PIP_{mt} from multitrait BayesRC genome-wide fine-mapping, highlighting variants with important functional annotations. The dashed line indicates a PIP_{mt} = 0.25. (*D*) Heat map of the cattle variants with significant pleiotropic effects that also had CADD predicted deleterious variants (Harmful). Hierarchical clustering was applied to variant effects on traits, and the numbers on top indicate the result of clusters. The color scale in cells indicates trait-specific PIP estimates from the multitrait BayesRC analysis; + indicates effects that are positive on the trait; − indicates effects that are negative on the trait; CAGE indicates variants annotated as enhancers by Capped Analysis of Gene Expression (CAGE) assays; BiBtDiff indicates variants with significant differences in allele frequencies between *Bos indicus* and *Bos taurus* subspecies; HiC indicates variants with chromatin interactions based on Chromosome Conformation Capture (39).

phenotypes in both species but had opposite evolutionary paths due to very different (epi)genomic selection forces. A full list of these potentially causal variants can be found in Dataset S3.

FAEMI Score Enhances Genome Prediction of Heat Tolerance. To validate the FAEMI score, it was applied to a different dataset with heat tolerance phenotypes from cattle. A detailed description of these heat tolerance traits can be found in previous studies (13–15, 42). Briefly, these traits were derived from the decline of milk, fat, protein, and lactose yield due to high temperature and humidity in (~42,000) Holstein cows, labeled HeatTol.milk, HeatTol.fat, HeatTol.prot and HeatTol.lact, respectively. 1.8 million LD pruned sequence variants in these cows were divided into three classes based on their FAEMI score: high-FAEMI (627,502 variants), medium-FAEMI (627,501 variants), and low-FAEMI (627,501 variants). Then, these 3 classes of variants were analyzed by BayesR (5, 43) and the effects of these sets of variants, trained in those 42,000 cows, were used to predict heat tolerance phenotypes in ~4,200 bulls with matching heat tolerance phenotypes.

The analysis of heat tolerance phenotypes with (adjusted) and without (raw) fitting the original milk production traits as fixed effects was evaluated (*Methods* and Fig. 4). As well as the performance of FAEMI score trained by the Random Forest machine learning method, the previous FAETH score and the random score (*Methods*). Across all scenarios, the FAEMI score provided the strongest discrimination in genomic prediction accuracy between high, medium, and low-ranking variants. In the raw analysis, high-FAEMI variants had a relative increase in prediction accuracy of 13 to 21% (average=16.7%, calculated as $\frac{r_{high}-r_{low}}{r_{low}}$), compared to low-FAEMI variants (Fig. 4*A*). Random Forest trained FAEMI score had a relative increase in prediction accuracy of 5 to 13% (average = 8.5%) while FAETH score had a relative increase in prediction accuracy of 5.2 to 5.5% (average = 5.3%) (Fig. 4*A*). In the adjusted analysis high-FAEMI variants had a relative increase of 8-13% (average = 11%) in explaining the additional phenotypic variance, after fitting milk traits as fixed effects, compared to low-FAEMI variants (Fig. 4*B*). Random Forest trained FAEMI score had a relative increase of 1 to 16% (average = 7%) in explaining the additional phenotypic variance, while FAETH score had a relative increase of –4 to 9% (average = 3.7%) in explaining the additional phenotypic variance. Therefore, our results show that the FAEMI score was informative in finding causal variants that enhance genomic selection of heat tolerance in cattle.

To further explore the utility of FAEMI score in improving genomic prediction accuracy, we compared the genomic prediction accuracy of heat tolerance traits with and without using the FAEMI score as a biological prior, i.e., BayesRC (40) VS BayesR. There was a relative increase of 3-11% (average = 7%) in prediction accuracy by using FAEMI as a prior (BayesRC), compared to not using FAEMI as a prior (BayesR) (Table 1). This further supports that Bayesian genome-wide analysis instructed by FAEMI is more informative. To test the usefulness of FAEMI score in a wider sample of cattle breeds, we partitioned the heritability of nine beef traits (average sample size of 2,710, Dataset S4) into SNP classes of FAEMI-high, medium, and low classes (*Methods*). Averaged across these nine beef traits, compared with low-FAEMI SNPs, FAEMI-high and FAEMI-medium SNPs explained significantly more heritability [24% (SE = 4.8%) and 15.3% (SE = 2.6%), respectively, *SI Appendix*, Fig. S4]. These results suggest that FAEMI score is also useful in finding informative variants in wider breeds and may improve genomic prediction in those breeds.

We then examined the top variants prioritized by BayesRC and BayesR together with their functional annotations. Consistent with the above results, top candidates were better mapped using FAEMI-informed BayesRC. One variant (Chr12:14623573 or rs383130643) had a BayesRC PIP of 0.79 associated with heat tolerance for milk (Fig. 5*A*), and BayesR PIP of 0.43 (Fig. 5*B*). Chr12:14623573/rs383130643 was located in a CAGE-annotated enhancer region (Fig. 5*C*) within the intronic region of the gene

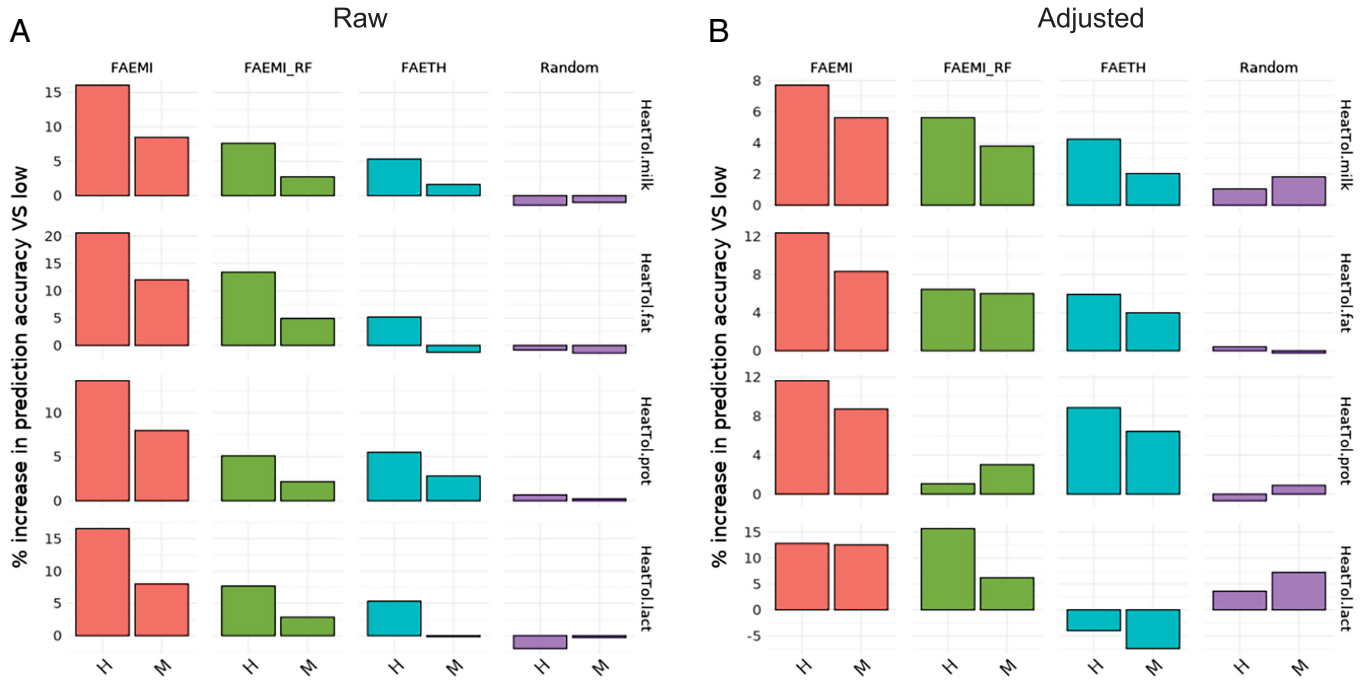

Fig. 4. Validation of FAEMI score. (*A*) Relative increase in genomic prediction accuracy (Pearson correlation between gEBV and phenotype) for heat tolerance traits compared with low-ranking variants. The label H indicates high-ranking FAEMI variants and label M indicates middle-ranking variants; FAEMI_RF indicates FAEMI score trained using Random Forest; FAETH indicates our previously developed variant ranking (8); Random indicates classification using random variants. (*B*) Relative increase in genomic prediction accuracy (additional phenotypic variance of heat tolerance traits explained by gEBV) after fitting the corresponding milk production traits as fixed effects for heat tolerance traits compared with low-ranking variants.

Table 1. Comparing genomic prediction accuracy of heat tolerance traits using FAEMI as a prior (BayesRC) and not (BayesR)

Trait	Method	Accuracy (R^2)	Relative increase (%)
HeatTol.fat	BayesRC	0.115	6.94
	BayesR	0.107	
HeatTol.lact	BayesRC	0.083	11.2
	BayesR	0.075	
HeatTol.milk	BayesRC	0.151	6.6
	BayesR	0.141	
HeatTol.prot	BayesRC	0.175	3.0
	BayesR	0.170	

Accuracy is the additional phenotypic variance in heat tolerance traits explained by gEBV after being adjusted for milk production traits. Relative increase is calculated as $(R^2_{BayesRC} - R^2_{BayesR})/R^2_{BayesR}$.

stress-associated endoplasmic reticulum protein family member 2 (*SERP2*), with reported links to cellular stress (44). Chr12:14623573/rs383130643 is under multiple ChIP-seq marks (Dataset S5) and is detected as a multigene and tissue significant eQTL (meta-analysis across 16 tissues, Dataset S6) (25). Still, its single-gene or tissue significance of eQTL mapping did not reach the declared threshold ($P = 5 \times 10^{-6}$). However, Chr12:14623573/rs383130643 was also a significant aseQTL for *SERP2* (Fig. 5*D*). Another variant Chr25:28127643 (rs876577204), had a BayesRC PIP of 0.71 associated with heat tolerance for lactose (Fig. 5*E*) and its BayesR PIP = 0.67 (Fig. 5*F*). Chr25:28127643/rs876577204 is also only a multigene and tissue *cis* eQTL with the strongest effects (from meta-analysis across tissues) in the rumen, muscle, and blood cells (Fig. 5*G*). It is located in the gene tyrosylprotein sulfotransferase 1 (*TPST1*) with reported links to shear stress (45) and is a significant aseQTL for *TPST1* (Fig. 5*H*). A full list of potential causal variants for heat tolerance traits can be found in Dataset S6.

Discussion

The FAEMI score combines many annotations of variants to predict the probability that they affect one or more of the 16 traits we analyzed. Compared to our previous study (FAETH score) (8), the derivation of the FAEMI score uses much bigger datasets (nearly 3 times larger training data for genotype-to-phenotype associations and 25 times more animals with functional data). Also, we analyze multiple traits jointly using Bayesian methods, which account for LD and phenotypic correlations. Regressing Bayesian probability of a variant affecting multiple phenotypes on functional annotations together with LD and MAF, FAEMI analyses further correct the ranking for these confounders. Joint analysis of annotations also accounts for the relationships between variants in different annotations, i.e., some variants and their LD mates could have multiple annotations. However, our results show LD and MAF had little impact on the phenotypic importance ranking of functional annotations. This is consistent with our previous work (8). As a result, the FAEMI score significantly outperforms the FAETH score in improving genomic prediction accuracy in external data, demonstrating its robust utility in improving the mapping and prediction of complex traits. In addition, we found that our multiple linear regression trained FAEMI score has significant advantages over the Random Forest machine learning trained FAEMI score in improving genomic prediction accuracy. This is consistent with recent reports where traditional predictive models are at least as good as Machine Learning models for analyses related to genomic prediction (46, 47).

Variants with more functional annotations tended to have a higher probability of association with more than one trait. Although to our knowledge this has not been reported, given that many of the annotations used here across populations can be viewed as molecular phenotypes [e.g., eQTLs (20) and hQTLs (28)], the convergence of pleiotropy at molecular and phenotypic levels could be expected. There is correlated information between different annotations, so fitting annotations all in one model reduces their importance compared to fitting them individually (Fig. 2*C*). However, regardless of the modeling method, variants associated with metabolic profiles (mQTL) and variants with regulatory roles in transcriptomic (e/sQTL and ase) and epigenomic (asb/hQTL) mechanisms had high importance.

Although variants conserved across species had significant phenotypic effects, different from our previous study (8), their effect sizes were small. Along with correlated information content between annotations as described above, the current study included many more types of functional categories and each of them had a substantially greater number of biological replicates, and this may have diluted the individual contribution of conserved sites to the phenotypic variance. In addition, the current study has more stringent corrections for LD and MAF. These improvements may have led to differences in rankings of functional annotations compared to our previous work (8).

Variants segregating in both humans and cattle have been reported (48). However, we found a handful of variants whose orthologs were predicted by CADD as deleterious in humans, associated with cattle traits (Fig. 3*C*). These variants had significantly different MAF spectra in cattle and humans, and this suggests these variants experienced very different selection during evolution. Interestingly, cattle variant Chr14:64454721 or rs445616049 significantly associated with milk, fat, and fertility phenotypes is also associated with Cohen syndrome in humans, which results in obesity phenotypes. It would be interesting to investigate whether the human ortholog variants of Chr14:64454721 or rs445616049 have protective effects on lactation and fertility in humans. If the same mutation has effects in humans and cattle, it increases the evidence that this mutation is causal in both species.

The FAEMI score was validated using new data with heat tolerance phenotypes. The heat tolerance phenotype used is an example of genetics-by-environment interaction because it measures how much milk yield declines as the temperature and humidity rise. Tested in various modeling approaches, high-FAEMI variants consistently had higher genomic prediction accuracy of heat tolerance than low-FAEMI variants. These results support the validity of the FAEMI ranking and also suggest that FAEMI score can assist in the selective breeding of thermal-tolerant cattle, as higher genomic prediction accuracy leads to more efficient breeding (49, 50). Also, we highlighted Chr12:14623573/rs383130643 located in *SERP2* significantly associated with heat tolerance for milk yield and Chr25:28127643/rs876577204 located in *TPST1* associated with heat tolerance for lactose. Both *SERP2* and *TPST1* have physiological links to stress responses (44, 45). Chr12:14623573/rs383130643 was annotated as an enhancer (Fig. 5*c*), suggesting that this mutation could be involved in epigenetic regulation. Therefore, these results are consistent with the theory that epigenetic regulation is significantly associated with gene-by-environment interactions (51).

While we provided a proof-of-concept study that supported the usefulness of FAEMI score in capturing heritability of beef cattle traits (*SI Appendix*, Fig. S4), future studies using a compiled annotation dataset to train FAEMI score with phenotypes from other cattle breeds will also be important. This will further validate the

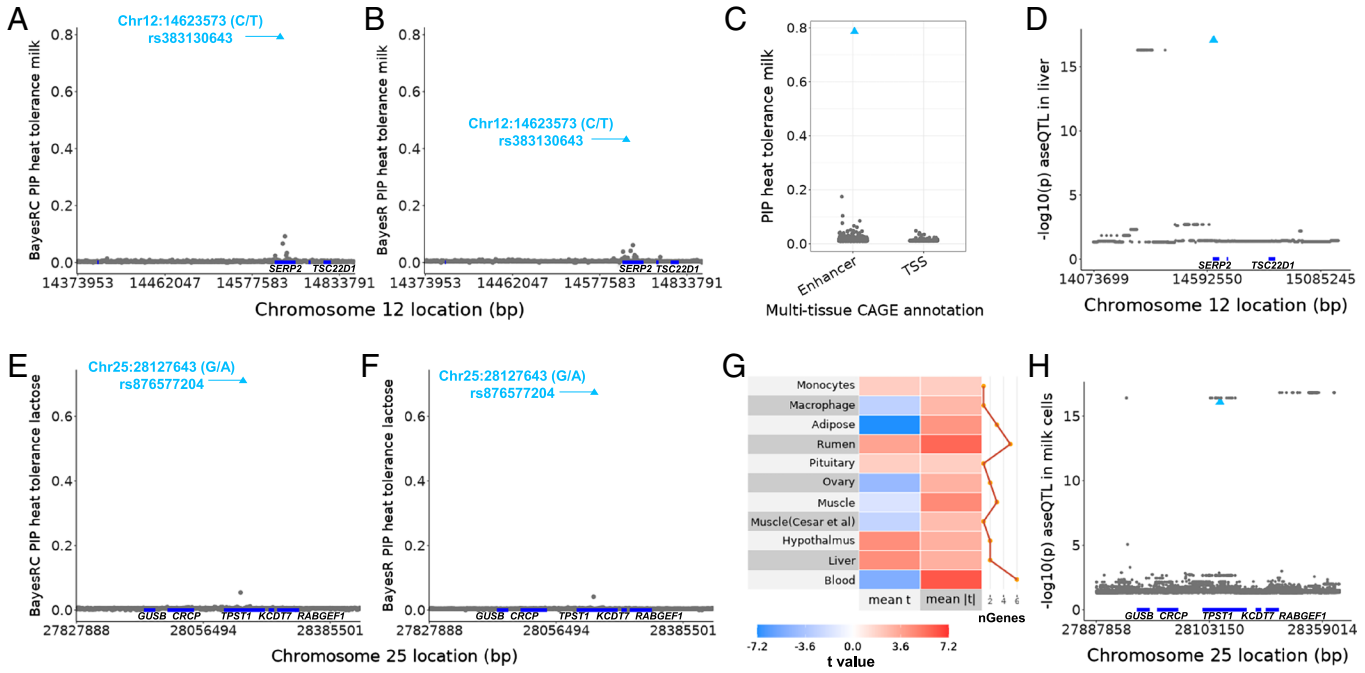

Fig. 5. Examples of fine-mapping and annotation for heat tolerance traits. (*A*) BayesRC mapping (posterior inclusion probability or PIP) for heat tolerance with milk yield for the region surrounding Chr12:14623573 (rs383130643, blue triangle) within stress-associated endoplasmic reticulum protein family member 2 (*SERP2,* genes indicated by blue lines in the x-axis). For all association tests, C is the effect allele of Chr12:14623573/rs383130643 and T is the alternative allele. (*B*) BayesR mapping for heat tolerance with milk yield for the region surrounding Chr12:14623573. (*C*) Distribution of BayesRC PIP across Capped Analysis of Gene Expression (CAGE) annotations of multiple cattle tissues. (*D*) Allele-specific expression QTL (aseQTL) mapping results from liver near the *SERP2* region. The blue triangle highlights the effect of Chr12:14623573/rs383130643 as an aseQTL for *SERP2*. (*E*) BayesRC mapping of heat tolerance with lactose yield for the region surrounding Chr25:28127643 (rs876577204, blue triangle) within tyrosylprotein sulfotransferase 1 (*TPST1*). For all association tests, G is the effect allele of Chr25:28127643/rs876577204 and A is the alternative allele. (*F*) BayesR mapping of heat tolerance with lactose yield for the region surrounding Chr25:28127643. (*G*) Effects of Chr25:28127643 on gene expression from the eQTL meta-analysis of different cattle tissues. Each cell is the t value (beta/se) of the variant in the meta-analysis, which tests whether the variant has an effect in at least one gene across 16 tissues (25). The number of genes (nGenes) affected per tissue is shown in the line graph. (*H*) Allele-specific expression QTL (aseQTL) mapping results from milk cells near the *TPS1* region. The blue triangle highlights the effect of Chr25:28127643/rs876577204 as an aseQTL for *TPS1*.

potential of FAEMI score to enhance genomic selection in more cattle breeds. While we showed that potential causal variants could impact the phenotype via molecular pathways, future research is needed to disentangle the potential causal relationships between different annotations (e.g., eQTLs) and heat tolerance traits to better understand the molecular drivers of thermal tolerance.

In conclusion, we developed the FAEMI framework, which combines the information from variant-phenotype associations and variant-function assays to rank genome-wide variants. FAEMI analyses inform future annotation experiments, prioritize informative variants, elucidate biological mechanisms behind complex traits across species and enhance selective breeding for resilient animals in the changing environment. FAEMI framework and variant scores are valuable methods and resources to better understand mammalian complex traits and achieve sustainable agriculture.

Methods

Australian Animals and Phenotype Data. Data were collected by farmers and processed by DataGene Australia (http://www.datagene.com.au/) for the official May 2020 release of national breeding values. No live animal experimentation was required. DataGene provided the bull and cow phenotypes as deregressed breeding values or trait deviations for cows, and daughter trait deviations for bulls (i.e., progeny test data for bulls). DataGene corrected the phenotypes for herd, year, season, and lactation following the procedures used for routine genetic evaluations in Australian dairy cattle. Phenotype data included a total of 103,350 animals, including Holstein (6,886♂/87,003♀), Jersey (1,562♂/13,353♀), crossbreed (36♂/5,037♀), and Australian Red (265♂/3,379♀) dairy breeds. In the FAEMI analysis, cows were used as the training set and bulls were used as the validation set. In total, 16 traits were studied that related to milk production, mastitis, fertility, temperament, and body conformation and the details of these traits can be found in Dataset S2. As these traits were to be analyzed by multitrait BayesR (24) which requires decorrelated traits, we applied the previously established Chelosky transformation (3, 52) to decorrelate these 16 traits. After decorrelation, the average Pearson correlation *r* between all trait pairs was −0.0076 (SD = 0.0199).

Genotype Data. The genotype data for Australian cows consisted of 16,251,453 sequence variants imputed using Run7 of the 1,000 Bull Genomes Project (21, 53). The details of the imputation were described previously (16, 54). Briefly, the imputation of biallelic sequence variants was performed with Minimac3 (55, 56) and those variants with imputation accuracy $R^2 > 0.4$ and minor allele frequency (MAF) > 0.005 in both bulls and cows were kept. The choice to use imputation accuracy $R^2 > 0.4$ was based on our empirical studies (57, 58), which supports this cutoff as the best for sequence analyses in cattle. Bulls were genotyped with either a medium-density SNP array (50 K: BovineSNP50 Beadchip, Illumina Inc) or a high-density SNP array (HD: BovineHD BeadChip, Illumina Inc) and cows were genotyped with the BovineSNP50 Beadchip (Illumina Inc) and a low-density customized panel. The genotype data for CattleGTEx animals were generated previously (20) and included a total of more than 6 million sequence variants imputed also using Run7 of the 1,000 Bull Genomes Project keeping variants with the imputation dosage R-squared > 0.8 and MAF > 0.001.

Functional and Evolutionary Data. Different datasets were collected, assembled, and analyzed to extract functional and evolutionary information as described in Dataset S1. Details of these datasets are described in *SI Appendix, Methods*.

Multitrait BayesR. The first analysis was a multitrait BayesR without any biological priors (no classes). All Bayesian analyses used the implementation of BayesR3 (43) using data from 16 decorrelated traits with more than 5 million pruned or clumped sequence variants. The pruning from 16 to 5 million variants used plink1.9 with LD-$r^2 > 0.995$ in 1 Mb windows and the clumping (described later) also used these two parameters. The model uses the general BayesR model as detailed below:

$$y = \mathbf{X}b + \mathbf{W}v + e, \quad [\mathbf{1}]$$

where y = vector of n cow phenotypes, b = vector of p fixed effect solutions, **X** = design matrix allocating phenotypes to fixed effects (X = n by p matrix), v = vector of m SNP effects, **W** = design matrix of SNP marker genotypes (n by m matrix), and e = vector of n residual errors, distributed N(0, $\mathbf{E}\sigma^2$e), where σ^2e = error variance and **E** = is a diagonal matrix constructed as diag($1/w_i$), where w_i is the weighting coefficient for each animal. Weighting coefficients were calculated differently for cows following Eqs. **2** and **3** of Garrick et al. (59), with the heritability of each trait determined by GREML, implemented using MTG2 [Lee and Van der Werf (60)]. The pedigree was not fitted. Different from ordinary BayesR, multitrait BayesR estimates a multitrait posterior inclusion probability (PIP_{mt}) or Q2 value for each SNP which is the probability that this variant is associated with at least one of the analyzed traits. As a validation, we also applied the same multitrait BayesR for the same 16 traits from 9 k bulls (Dataset S2).

Multiple Regression of Q2 on Functional and Evolutionary Classes. The following multiple regression was used to jointly analyze all functional and evolutionary classes (see detailed explanation of these classes in the *SI Appendix*):

$$\begin{aligned} Q2 = {} & intercept + VEP + FAANG.ChIP + CAGE + HiC \\ & + AnimalQTLdb + cGTEx.eQTL + cGTEx.sQTL + aseQTL \\ & + asbQTL + hQTL + LCMS.mQTL + NMR.mQTL + SNP.age \\ & + Species.diff + Conserved + Human.harmful + LD \\ & + MAF + SNP.density + e, \end{aligned} \quad [\mathbf{2}]$$

where *Q2* was the PIP_{mt} from multitrait BayesR on 5 M variants; *VEP* was a factor consisting of 9 levels of UTR, coding.related, gene.end, intronic, missense, non.coding.related, splice.site, synonymous and intergenic; *FAANG.ChIP* was factor including 4 levels of Annotated.1study, Annotated.2studies, Annotated.3studies, and the remaining variants; *CAGE* was a factor including 4 levels of Enhancer&Super.enhancer, TSS, super.enhancer, and remaining variants; *HiC* was a factor including 3 levels of topActive, topRepressed, and remaining variants; *AnimalQTLdb* was a factor including 2 levels of annotated and the remaining variants; *cGTEx.eQTL* was a factor including 3 levels of cis.eQTL, cistrans.eQTL, and remaining variants; *cGTEx.sQTL* was a factor including 3 levels of cis.sQTL, cistrans.sQTL, and remaining variants; *aseQTL* was a factor including two levels of cis.aseQTL and remaining variants; *asbQTL* was a factor including 4 levels of H3K4Me1.asbQTL, H3K4Me3.asbQTL, Multiple.mark.asbQTL, and remaining variants; *hQTL* was a factor including 3 levels of H3K4Me3.hQTL, Multiple.mark.hQTL, and remaining variants; *LCMS.mQTL* was a factor including 2 levels of LCMS.mQTL and remaining variants; *NMR.mQTL* was a factor including 2 levels of NMR.mQTL and remaining variants; *SNP.age* was a factor including 2 levels of young and remaining variants; *Species.diff* was a factor including 2 levels of Indicus.rare and remaining variants; *Conserved* was a factor including 5 levels of Cons100v, Cons100v30m, Cons200m, Cons30m, and remaining variants; *Human.harmful* was based on Combined Annotation Dependent Depletion or CADD score on the human genome (see Supplementary information) and was a factor including 3 levels of Allele.matched, Non.allele.matched, and remaining variants; *LD* was a continuous variable of LD score of each variant; MAF was a continuous variable of minor allele frequency; SNP.density was a continuous variable of the number of SNPs in the LD scoring window; *e* was the error term. For the factor of VEP, the reference level was set to intergenic and for other factors, the reference level was set to the remaining variants. See Dataset S1 and the above Method sections for details of functional classes and levels. Functional and evolutionary classes on all 16 million variants are publicly available at https://figshare.unimelb.edu.au/articles/dataset/Functional-And-Evolutionary_Multi-trait_Importance_FAEMI_score_for_16_million_sequence_variants/27160245?file=58912450.

As a comparison, we also trained FAEMI score following the suggestion from Wang et al. (10). The same set of response and explanatory variables listed in Eq. **2** were analyzed by Random Forest implemented in the R package (v4.0.0) "ranger" in the same training data. The number of trees was set to 2000, other parameters used the default setting. Then, FAEMI score was repredicted based on the coefficients from the Random Forest training.

Functional-And-Evolutionary Multi-trait Importance, FAEMI score. Using regression coefficients obtained from Eq. **1**, we made predictions of FAEMI score all variants given their membership of functional and evolutionary classes, i.e., design matrix:

$$FAEMI\ score = \Phi\hat{\varepsilon}, \quad [\mathbf{3}]$$

where Φ was the design matrix of functional and evolutionary classes, where factors had cell values of either 1 or 0, and $\hat{\varepsilon}$ was the effects or regression coefficients of functional and evolutionary classes estimated from Eq. **1**. While we have adjusted MAF and LD in estimating $\hat{\varepsilon}$, in predicting FAEMI score, we excluded the effects of MAF and LD because we did not want to bias the score based on these.

FAEMI Score Strata Used in Multitrait BayesRC. With the FAEMI score estimated for 16 million sequence variants, we performed LD clumping using plink1.9 (61) with LD-$r^2 > 0.995$ in 1 Mb windows for the first 1-3 quartiles of variants (12,182,274 variants). The clumping using the FAEMI score led to 4,125,432 variants and we divided them into 4 strata where the 1st strata had the highest FAEMI score and the 4th strata had the lowest FAEMI score. For the 3,853,170 (out of the total 16 M) variants that ranked in the 4th quartile of FAEMI score, we conducted pruning with LD-$r^2 > 0.995$ in 1 Mb windows. This is because this set had little information on the FAEMI score to prioritize variants. The pruning of this set of variants led to 1,238,711 variants. Combining the results from clumping and pruning led to a total of 5,364,143 variants within 5 strata where the 1st strata had 1,040,404 variants, the 2nd, 3rd, 4th, and 5th strata had 1,033,994, 1,031,806, 1,019,228, and 1,238,711 variants respectively. Then, these five groups were used as variant priors in BayesRC to analyze the same data as described in Eq. **1**. BayesRC divides the variants into classes ("*c*", here $c = 5$) according to prior biological information and estimates the mixing proportions of the four normal distributions separately for each class of variants. The BayesRC (62) model used here for association analysis of phenotypes was

$$y_{P_M} = \mathbf{W}v + \mathbf{X}b + e, \quad [\mathbf{4}]$$

where y_{P_M} was the vector of corrected phenotypes for a given trait, **W** was the design matrix of marker genotypes, centered and standardized to have a unit variance, *v* was the vector of variant effects, **X** was the design matrix allocating phenotypes to fixed effects, and *b* was the vector of fixed effects. As a result of 50,000 iterations with 25,000 burn-ins of Markov chain Monte Carlo (MCMC) with 10 independent chains tested, the effect *v* for each variant jointly estimated with other variants was obtained. This mixture of distributions is modeled independently in each class of variants to allow for different mixture models per class ("*c*").

Validation Using Heat Tolerance Data. We used the heat tolerance phenotypes of cattle for validation. Detailed descriptions of heat tolerance traits can be found in previous studies (13–15, 42), but briefly, these traits were derived from the decline of milk, fat, protein, and lactose yield due to high temperature and humidity in Holstein cows, labeled HeatTol.milk (N = 41,028), HeatTol.fat (N = 41,028), HeatTol.prot (N = 41,028), and HeatTol.lact (N = 29,320), respectively. We also used data from Holstein bulls as a validation dataset for genomic prediction of heat tolerance as described later [HeatTol.milk (N = 4,136), HeatTol.fat (N = 4,136), HeatTol.prot (N = 4,136), and HeatTol.lact (N = 3,009)]. The derivation used reaction norm models based on the temperature–humidity index (THI). The weather data from 2001 to 2021 comprised hourly measures of dry bulb temperature and relative humidity obtained from the Bureau of Meteorology (Melbourne, Australia) for 474 weather stations located in 6 different states of Australia. The information on the location of each dairy herd was obtained from DataGene to match with the respective weather station. In total, we matched 136 stations to 10,694 herds, which are within 60 km of the respective closest weather stations.

We used the genotype dataset described previously (25) which were 1,882,504 LD pruned ($r^2 < 0.9$) variants imputed using Run7 of the 1,000 Bull Genomes Project (21, 53). The details of the imputation were described previously (63). Briefly, the imputation of biallelic sequence variants was performed with Minimac3 (55, 56) and those variants with imputation accuracy $R^2 > 0.4$ and minor allele frequency (MAF) > 0.005 in both bulls and cows were kept. These 1,882,504 variants were divided into three classes using FAEMI score: high-FAEMI (627,502 variants), medium-FAEMI (627,501 variants), and low-FAEMI (627,501 variants). Then, these 3 classes of variants were jointly analyzed by

BayesRC (40, 43) to partition genetic variances in cows. Also, we trained BayesR (5, 43) effects of FAEMI-high and FAEMI-low variants separately in cows and used these to predict heat tolerance phenotypes in bulls. This would allow the comparison of genomic prediction accuracy of heat tolerance traits between FAEMI-high and FAEMI-low variants. In both BayesRC and BayesR analyses, we evaluated analyzing heat tolerance phenotypes with and without fitting the original milk production traits as fixed effects, e.g, fitting milk yield as a fixed effect when analyzing HeatTol.milk, to account for the correlation between heat tolerance and original phenotypes. The analysis of heat tolerance without fitting original milk production traits as fixed effects was labeled as "raw," whereas the analysis of heat tolerance fitting original milk production traits as fixed effects was labeled as "adjusted."

Bayes R models the prior distribution of variant effects as a mixture of four normal distributions including a null distribution, zero-effect [$N(0, 0.0\sigma^2_g)$], and three others: small-effect [$N(0, 0.0001\sigma^2_g)$], medium-effect [$N(0, 0.001\sigma^2_g)$] and large-effect [$N(0, 0.01\sigma^2_g)$], where σ^2_g is the additive genetic variance for the trait. Partitioning heritability using BayesRC followed previous protocols (25). The model of BayesRC is the same as Eq. **4** described above, however the variant priors are three classes: high-, medium-, and low-FAEMI score ($c = 3$). In the raw analysis, the heritability of four heat tolerance traits was 0.185 for HeatTol.fat, 0.223 for HeatTol.lact, 0.228 for HeatTol.milk and 0.188 for HeatTol.prot. In the adjusted analysis, the heritability of four heat tolerance traits was 0.093 for HeatTol.fat, 0.094 for HeatTol.lact, 0.1 for HeatTol.milk and 0.139 for HeatTol.prot.

We evaluated using BayesR to train high-FAEMI variants and low-FAEMI variants separately in cows and predict the heat tolerance traits in bulls. This means that for each heat tolerance trait, BayesR effects for high-FAEMI variants and low-FAEMI variants were generated separately to estimate high-FAEMI-gEBV and low-FAEMI-gEBV, of which the accuracy was tested in bulls. The modeling approach of BayesR is similar to BayesRC but without the variant classes. Where BayesR gEBV of heat tolerance were obtained after fitting milk production traits in cows ("adjusted" as described above), in the prediction in bulls, we estimated the additional phenotype variance explained by gEBV. This was done by first fitting a baseline model

$$y_{HeatTol} = milk\_traits + e, \quad [5]$$

to estimate the R^2_1; and fitting a secondary model

$$y_{HeatTol} = milk\_traits + gEBV_{HeatTol} + e, \quad [6]$$

to estimate R^2_2. The additional phenotype variance explained by gEBV or $\Delta R = R^2_2 - R^2_1$. ΔR was estimated for both gEBV calculated using high-FAEMI variant and low-FAEMI variant effects trained by BayesR.

Analyses of Beef Cattle Traits. The nine beef phenotypes used were a subset of a previous study (64), covering body weight, muscle mass, intramuscular fat, carcass yield, and marbling score (Dataset S4). Breeds of Angus, Murray Gray, and Hereford were used. Genotypes included 729,068 SNPs from the bovine High-density panel. SNPs were categorized into FAEMI-high, medium, and low and were analyzed by BayesRC using Eq. **4**. Partitioning heritability followed previous protocols (25). Briefly, first, the following equation was used:

$$V_{a_{class}} = V_a \times N_{s_{class_i}} \times 0.01\,\% + V_a \times N_{m_{class_i}} \times 0.1\,\% + V_a \times N_{l_{class_i}} \times 1\,\%, \quad [7]$$

where $N_{s_{class_i}}$ was the number of small-effect variants in class i (e.g., high-FAEMI SNPs), $N_{m_{class_i}}$ was the number of medium-effect variants in high-FAEMI SNPs, and $N_{l_{class_i}}$ was the number of large-effect variants in high-FAEMI SNPs. Then, for each class, we used

$$h^2 = \frac{V_a}{(V_a + V_e)}, \quad [8]$$

to calculate h^2 for each class ($h^2_{class_i}$), and then, the observed proportion of h^2 explained by each class as

$$h^2_{class_i}\,\% = \frac{h^2_{class_i}}{\sum_1^{N.class} h^2_{class_i}}, \quad [9]$$

where $N.class$ was the total number of classes fitted in the model. We derive an expected $h^2_{class_i}\,\%$, or $E(h^2_{class_i}\,\%)$ using the $h^2_{class}\,\%$ and the proportion of variants for the remaining class (low-FAEMI or non-FAEMI SNPs):

$$E(h^2_{class_i}\,\%) = \frac{h^2_{class_{remaining}}\,\%}{Variants_{class_{remaining}}\,\%} \times Variants_{class_i}\,\%. \quad [10]$$

The difference between observed heritability explained and expected heritability explained is interpreted as more heritability explained than expected.

Data, Materials, and Software Availability. The FAEMI variant scores and all annotation categories are publicly available at https://figshare.unimelb.edu.au/articles/dataset/Functional-And-Evolutionary_Multi-trait_Importance_FAEMI_score_for_16_million_sequence_variants/27160245?file=58912450, which is accompanied by detailed explanations and tutorials. The Hi-C data (raw sequence) are available as part of the FAANG consortium via European Nucleotide Archive (ENA) under the biosample accessions of SAMEA4675143, SAMEA4447814, and SAMEA4447787, under the study accession of ERP182606. CAGE data are available via the ENA under study ID PRJEB43513 and PRJEB44817, respectively (65). The FAANG ChIP-seq data can be obtained via publications (31–33). RNA-seq data related to e/sQTL mapping can be accessed via the CattleGTEx consortium: http://cgtex.roslin.ed.ac.uk/. Linear mixed model-based summary statistics of mapped eQTLs and sQTLs from each of the 16 tissues and the multitissue analysis are available at figshare: https://melbourne.figshare.com/articles/dataset/eQTL_and_sQTL_from_16_cattle_tissues_linear_mixed_model_/19793047. The RNA-seq data related to aseQTL mapping are published via NCBI SRA with accession number PRJNA682457; ChIP-seq data related to hQTL and asbQTL mapping are available via ENA with accession number PRJEB52456 (28). The human CADD score can be found at https://cadd.gs.washington.edu/. The DNA sequence data as part of the 1,000 Bull Genomes Consortium are available to consortium members. Sequence data from the 1,000 Bull Genome Project have been made publicly available at EBI: https://www.ebi.ac.uk/eva/?eva-study=PRJEB42783. DataGene Limited (http://www.datagene.com.au/) manages the raw phenotype and genotype data of Australian dairy animals, and access to these data for research purposes may be granted upon request to DataGene. Other supporting data are shown in the Supplementary Materials of the manuscript. No original computer codes are generated in the current study. The linear mixed model analysis used GCTA (66). Bayesian analysis used BayesRC (40, 43).

ACKNOWLEDGMENTS. The Australian Research Council's Discovery Projects (DP160101056, DP200100499, and DP230101352) supported R.X. and M.E.G. DairyBio, a joint venture project of Agriculture Victoria (Melbourne, Australia), Dairy Australia (Melbourne, Australia), and the Gardiner Foundation (Melbourne, Australia), funded computing resources used in the analysis. Liver samples, SNP, and other data from the NZ selection experiment were kindly provided by Drs. Susanne Meier, Chris Burke, and Claire Phyn (DairyNZ Ltd., Hamilton, NZ) and were collected under the Pillars of a New Dairy System research program, which was funded by NZ dairy farmers through DairyNZ Inc. (Hamilton, NZ) and by the Ministry of Business, Innovation and Employment (Wellington, NZ; contract number DRCX1302), with aligned AgResearch SIFF funding (Hamilton, NZ). We thank Dr. Iona M. Macleod for critical reviews of the manuscript. We also thank the University of Melbourne, Australia, for supporting this research. No funding bodies participated in the design of the study nor the analysis, interpretation of data, or writing of the manuscript. The 1,000 Bull Genomes consortium provided access to cattle sequence data, and the CattleGTEx consortium provided access to expression data.

Author affiliations: [a]Division of Genomics and Cellular Sciences, Agriculture Victoria, AgriBio, Centre for AgriBiosciences, Bundoora, VIC 3083, Australia; [b]School of Applied Systems Biology, La Trobe University, Bundoora, VIC 3083, Australia; [c]School of Agriculture, Food and Ecosystem Sciences, The University of Melbourne, Parkville, VIC 3052, Australia; [d]Cambridge-Baker Systems Genomics Initiative, Baker Heart and Diabetes Institute, Melbourne, VIC 3004, Australia; [e]SciLifeLab, Uppsala University, Uppsala 751 05, Sweden; [f]Department of Medical Biochemistry and Microbiology, Uppsala University, Uppsala 751 23, Sweden; and [g]Broad Institute of Massachusetts Institute of Technology and Harvard, Cambridge, MA 02142

1. E. Uffelmann *et al.*, Genome-wide association studies. *Nat. Rev. Methods Primers* **1**, 59 (2021).
2. A. Abdellaoui, L. Yengo, K. J. Verweij, P. M. Visscher, 15 years of GWAS discovery: Realizing the promise. *Am. J. Hum. Genet.* **110**, 179–194 (2023).
3. R. Xiang, I. van den Berg, I. M. MacLeod, H. D. Daetwyler, M. E. Goddard, Effect direction meta-analysis of GWAS identifies extreme, prevalent and shared pleiotropy in a large mammal. *Commun. Biol.* **3**, 1–14 (2020).
4. K. Watanabe *et al.*, A global overview of pleiotropy and genetic architecture in complex traits. *Nat. Genet.* **51**, 1339–1348 (2019).
5. M. Erbe *et al.*, Improving accuracy of genomic predictions within and between dairy cattle breeds with imputed high-density single nucleotide polymorphism panels. *J. Dairy Sci.* **95**, 4114–4129 (2012).
6. R. Maier *et al.*, Joint analysis of psychiatric disorders increases accuracy of risk prediction for schizophrenia, bipolar disorder, and major depressive disorder. *Am. J. Hum. Genet.* **96**, 283–294 (2015).
7. M. Ghoreishifar *et al.*, Allele-specific binding variants causing ChIP-seq peak height of histone modification are not enriched in expression QTL annotations. *Genet. Sel. Evol.* **56**, 50 (2024).
8. R. Xiang *et al.*, Quantifying the contribution of sequence variants with regulatory and evolutionary significance to 34 bovine complex traits. *Proc. Natl. Acad. Sci.* **116**, 19398–19408 (2019).
9. R. Zhao *et al.*, The potential of regulatory variant prediction AI models to improve cattle traits. bioXriv [Preprint] (2024), https://doi.org/10.1101/2024.08.01.606140 (Accessed 1 June 2025).
10. Q. S. Wang *et al.*, Leveraging supervised learning for functionally informed fine-mapping of cis-eQTLs identifies an additional 20, 913 putative causal eQTLs. *Nat. Commun.* **12**, 3394 (2021).
11. M. Ghoreishifar *et al.*, An integrative approach to prioritize candidate causal genes for complex traits in cattle. *PLoS Genet.* **21**, e1011492 (2025).
12. P. Thornton, G. Nelson, D. Mayberry, M. Herrero, Impacts of heat stress on global cattle production during the 21st century: A modelling study. *Lancet Planet. Health* **6**, e192–e201 (2022).
13. E. K. Cheruiyot, M. Haile-Mariam, B. G. Cocks, J. E. Pryce, Improving genomic selection for heat tolerance in dairy cattle: Current opportunities and future directions. *Front. Genet.* **13**, 894067 (2022).
14. T. T. Nguyen, P. J. Bowman, M. Haile-Mariam, J. E. Pryce, B. J. Hayes, Genomic selection for tolerance to heat stress in Australian dairy cattle. *J. Dairy Sci.* **99**, 2849–2862 (2016).
15. E. K. Cheruiyot *et al.*, New loci and neuronal pathways for resilience to heat stress in cattle. *Sci. Rep.* **11**, 16619 (2021).
16. R. Xiang *et al.*, Genome-wide fine-mapping identifies pleiotropic and functional variants that predict many traits across global cattle populations. *Nat. Commun.* **12**, 1–13 (2021).
17. M. Schubach *et al.*, 7: Using protein language models, regulatory CNNs and other nucleotide-level scores to improve genome-wide variant predictions. *Nucleic Acids Res.* **52**, D1143–D1154 (2024).
18. Z.-L. Hu, C. A. Park, J. M. Reecy, Bringing the Animal QTLdb and CorrDB into the future: Meeting new challenges and providing updated services. *Nucleic Acids Res.* **50**, D956–D961 (2022).
19. E. L. Clark *et al.*, From FAANG to fork: Application of highly annotated genomes to improve farmed animal production. *Genome Biol.* **21**, 1–9 (2020).
20. S. Liu *et al.*, A multi-tissue atlas of regulatory variants in cattle. *Nat. Genet.* **54**, 1438–1447 (2022).
21. H. Daetwyler *et al.*, Genomic prediction in animals and plants: simulation of data, validation, reporting, and benchmarking. *Genetics* **193**, 347–365 (2013)
22. H. D. Daetwyler *et al.*, Whole-genome sequencing of 234 bulls facilitates mapping of monogenic and complex traits in cattle. *Nat. Genet.* **46**, 858 (2014).
23. D. P. Genereux *et al.*, A comparative genomics multitool for scientific discovery and conservation. *Nature* **587**, 240–245 (2020), 10.1038/s41586-020-2876-6.
24. K. E. Kemper, P. J. Bowman, B. J. Hayes, P. M. Visscher, M. E. Goddard, A multi-trait Bayesian method for mapping QTL and genomic prediction. *Genet. Sel. Evol.* **50**, 10 (2018).
25. R. Xiang *et al.*, Gene expression and RNA splicing explain large proportions of the heritability for complex traits in cattle. *Cell Genomics* **3**, 100385 (2023).
26. R. Xiang *et al.*, Genetic score omics regression and multitrait meta-analysis detect widespread cis-regulatory effects shaping bovine complex traits. *PNAS Nexus* **4**, pgaf208 (2025), 10.1093/pnasnexus/pgaf208.
27. W. McLaren *et al.*, The ensembl variant effect predictor. *Genome Biol.* **17**, 122 (2016), 10.1186/s13059-016-0974-4.
28. C. P. Prowse-Wilkins *et al.*, Genetic variation in histone modifications and gene expression identifies regulatory variants in the mammary gland of cattle. *BMC Genomics* **23**, 815 (2022).
29. P. Rentzsch, D. Witten, G. M. Cooper, J. Shendure, M. Kircher, CADD: Predicting the deleteriousness of variants throughout the human genome. *Nucleic Acids Res.* **47**, D886–D894 (2019).
30. C. P. Prowse-Wilkins *et al.*, Putative causal variants are enriched in annotated functional regions from six bovine tissues. *Front. Genet.* **12**, 664379 (2021), 10.3389/fgene.2021.664379.
31. C. Kern *et al.*, Functional annotations of three domestic animal genomes provide vital resources for comparative and agricultural research. *Nat. Commun.* **12**, 1821 (2021), 10.1038/s41467-021-22100-8.
32. S. Foissac *et al.*, Multi-species annotation of transcriptome and chromatin structure in domesticated animals. *BMC Biol.* **17**, 1–25 (2019).
33. L. Fang *et al.*, Functional annotation of the cattle genome through systematic discovery and characterization of chromatin states and butyrate-induced variations. *BMC Biol.* **17**, 1–16 (2019).
34. J.-P. Fortin, K. D. Hansen, Reconstructing A/B compartments as revealed by Hi-C using long-range correlations in epigenetic data. *Genome Biol.* **16**, 1–23 (2015).
35. E. Lieberman-Aiden *et al.*, Comprehensive mapping of long-range interactions reveals folding principles of the human genome. *Science* **326**, 289–293 (2009).
36. J. B. Nielsen *et al.*, Biobank-driven genomic discovery yields new insight into atrial fibrillation biology. *Nat. Genet.* **50**, 1234 (2018).
37. L. Jiang *et al.*, A resource-efficient tool for mixed model association analysis of large-scale data. *Nat. Genet.* **51**, 1749–1755 (2019).
38. I. M. Kaplow *et al.*, Inferring mammalian tissue-specific regulatory conservation by predicting tissue-specific differences in open chromatin. *BMC Genomics* **23**, 1–23 (2022).
39. J.-M. Belton *et al.*, Hi–C: A comprehensive technique to capture the conformation of genomes. *Methods* **58**, 268–276 (2012).
40. I. MacLeod *et al.*, Exploiting biological priors and sequence variants enhances QTL discovery and genomic prediction of complex traits. *BMC Genomics* **17**, 1–21 (2016).
41. S. T. Sherry *et al.*, dbSNP: The NCBI database of genetic variation. *Nucleic Acids Res.* **29**, 308–311 (2001).
42. E. K. Cheruiyot *et al.*, Genotype-by-environment (temperature-humidity) interaction of milk production traits in Australian Holstein cattle. *J. Dairy Sci.* **103**, 2460–2476 (2020).
43. E. J. Breen *et al.*, Bayesr3 enables fast MCMC blocked processing for largescale multi-trait genomic prediction and QTN mapping analysis. *Commun. Biol.* **5**, 661 (2022), 10.1038/s42003-022-03624-1.
44. L. Iuliano *et al.*, Proteotoxic stress-induced apoptosis in cancer cells: Understanding the susceptibility and enhancing the potency. *Cell Death Discov.* **8**, 407 (2022).
45. S. Goettsch, W. Goettsch, H. Morawietz, P. Bayer, Shear stress mediates tyrosylprotein sulfotransferase isoform shift in human endothelial cells. *Biochem. Biophys. Res. Commun.* **294**, 541–546 (2002).
46. M. Kelemen *et al.*, Performance of deep-learning based approaches to improve polygenic scores. *Nat. Commun.* **16**, 5152 (2025).
47. P. Bellot, G. de Los Campos, M. Pérez-Enciso, Can deep learning improve genomic prediction of complex human traits? *Genetics* **210**, 809–819 (2018).
48. R. Zhao *et al.*, The conservation of human functional variants and their effects across livestock species. *Commun. Biol.* **5**, 1003 (2022).
49. T. H. Meuwissen, B. J. Hayes, M. Goddard, Prediction of total genetic value using genome-wide dense marker maps. *Genetics* **157**, 1819–1829 (2001).
50. J. C. Dekkers, H. Su, J. Cheng, Predicting the accuracy of genomic predictions. *Genet. Sel. Evol.* **53**, 1–23 (2021).
51. G. Cavalli, E. Heard, Advances in epigenetics link genetics to the environment and disease. *Nature* **571**, 489–499 (2019).
52. R. Xiang, I. M. MacLeod, S. Bolormaa, M. E. Goddard, Genome-wide comparative analyses of correlated and uncorrelated phenotypes identify major pleiotropic variants in dairy cattle. *Sci. Rep.* **7**, 9248 (2017).
53. H. Daetwyler *et al.* "Integration of functional genomics and phenomics into genomic prediction raises its accuracy in sheep and dairy cattle" in *Proceedings of the Association for the Advancement of Animal Breeding and Genetics, Armidale, NSW, Australia* (2019), pp. 11–14.
54. R. Xiang *et al.*, Genetic score omics regression and multi-trait meta-analysis detect widespread cis-regulatory effects shaping bovine complex traits. *PNAS Nexus* **4**, pgaf208 (2025).
55. C. Fuchsberger, G. R. Abecasis, D. A. Hinds, minimac2: Faster genotype imputation. *Bioinformatics (Oxford, England)* **31**, 782–784 (2014).
56. B. Howie, C. Fuchsberger, M. Stephens, J. Marchini, G. R. Abecasis, Fast and accurate genotype imputation in genome-wide association studies through pre-phasing. *Nat. Genet.* **44**, 955 (2012).
57. I. den Berg *et al.*, Imputation accuracy and carrier frequency of deleterious recessive defects in Australian dairy cattle. *J. Dairy Sci.* **107**, 9591–9601 (2024).
58. T. V. Nguyen *et al.*, Empirical versus estimated accuracy of imputation: Optimising filtering thresholds for sequence imputation. *Genet. Sel. Evol.* **56**, 72 (2024).
59. D. J. Garrick, J. F. Taylor, R. L. Fernando, Deregressing estimated breeding values and weighting information for genomic regression analyses. *Genet. Sel. Evol.* **41**, 55 (2009).
60. S. H. Lee, J. H. Van der Werf, MTG2: An efficient algorithm for multivariate linear mixed model analysis based on genomic information. *Bioinformatics* **32**, 1420–1422 (2016).
61. C. C. Chang *et al.*, Second-generation PLINK: Rising to the challenge of larger and richer datasets. *Gigascience* **4**, 7 (2015), 10.1186/s13742-015-0047-8.
62. I. MacLeod *et al.*, Exploiting biological priors and sequence variants enhances QTL discovery and genomic prediction of complex traits. *BMC Genomics* **17**, 144 (2016).
63. R. Xiang *et al.*, Mutant alleles differentially shape fitness and other complex traits in cattle. *Commun. Biol.* **4**, 1–10 (2021).
64. S. Bolormaa *et al.*, A Multi-Trait, Meta-analysis for Detecting Pleiotropic Polymorphisms for Stature, Fatness and Reproduction in Beef Cattle. *PLOS Genetics* **10**, e1004198 (2014), 10.1371/journal.pgen.1004198.
65. M. Forutan *et al.*, Evolution of tissue and developmental specificity of transcription start sites in *Bos taurus indicus*. *Commun. Biol.* **4**, 1–14 (2021).
66. J. Yang, S. H. Lee, M. E. Goddard, P. M. Visscher, GCTA: A tool for genome-wide complex trait analysis. *Am. J. Hum. Genet.* **88**, 76–82 (2011).